JOURNAL OF EARTHQUAKE ENGINEERING
2024, VOL. 28, NO. 8, 2310–2329
https://doi.org/10.1080/13632469.2023.2297849

Non-Dimensional Probabilistic Analysis of Seismic Pounding Between Flexible Structures and Rigid Boundaries

Domenico Altieri [a], Enrico Tubaldi [b], Michele Barbato [c], and Edoardo Patelli [b]

[a]Department of Environment Construction and Design, ISAAC, SUPSI, Mendrisio, Switzerland; [b]Department of Civil and Environmental Engineering, Strathclyde University, Glasgow, UK; [c]Department of Civil and Environmental Engineering, University of California Davis, Davis, California, USA

ABSTRACT

Pounding between adjacent structures subjected to earthquake actions can cause significant damage. Due to the many uncertainties inherent to the seismic input and the impact phenomenon, a probabilistic assessment of the occurrence of seismic pounding and of its consequences on the structural performance is necessary. This work analyzes the problem of pounding by considering a single-degree-of-freedom benchmark system surrounded by rigid boundaries and subjected to a stochastic earthquake input. Although simplified, the model is representative of several realistic configurations, such as base-isolated systems surrounded by moat walls or bridge decks near the bridge abutments. The problem is cast in non-dimensional form and a parametric study is carried out to evaluate the influence of the identified non-dimensional input parameters on the statistics of the response. A probabilistic demand model is developed for the impact forces via non-linear regression, with the demand expressed as a function of the identified non-dimensional parameters. This model provides an estimate of median pounding force and of its dispersion given the seismic intensity of the input. Finally, global sensitivity analysis is used to rank the model parameters in terms of their influence on the system performance.

ARTICLE HISTORY
Received 22 February 2022
Accepted 22 November 2023

KEYWORDS
Pounding; impact forces; dimensional analysis; probabilistic seismic demand model; risk assessment; sensitivity analysis

1. Introduction

Seismic events can lead to dynamic pounding between adjacent structural and/or non-structural systems characterized by a different dynamic response and insufficient separation distance (Anagnostopoulos 1988; Maison and Kasai 1992). Pounding has been reported to affect wide ranges of systems, such as buildings, bridges, and components of nuclear power plants (Altieri et al. 2020; Kim et al. 2015; Masroor and Mosqueda 2012; Nagarajaiah and Sun 2001; Otsuka et al. 1996). Seismic pounding can produce a wide range of effects, from isolated local damage to global collapse in case of strong earthquakes (Bertero 1987).

Adjacent buildings located in densely populated areas are structures at high risk of pounding (Anagnostopoulos and Spiliopoulos 1992; Bertero 1987; Moehle and Mahin 1991; Penzien 1997), because they tend to be in contact or at a close distance between each other. Increasing differences in vibration periods are usually associated to increasing risk of pounding (Anagnostopoulos and Spiliopoulos 1992). In general, dynamic impacts between buildings can lead to significant structural response amplifications, causing relevant permanent deformations due to yielding or, in extreme cases, catastrophic collapse for the

CONTACT Edoardo Patelli edoardo.patelli@strath.ac.uk Department of Civil and Environmental Engineering, Strathclyde University, 75 Montrose Street Glasgow, Glasgow G1 1XJ, UK

weaker buildings (Jankowski 2008). Moreover, when important non-structural elements (e.g. equipment and elevators) are affected, seismic pounding can result in a suspension or reduction of the serviceability of buildings, thus affecting the recovery process after the seismic event (Jeng and Tzeng 2000). Indeed, non-structural components can amount to between 60% (in residential buildings) and 92% (in hospitals) of the total construction expenses (Zito et al. 2022). Seismic pounding can also occur between base-isolated buildings and the surrounding moat walls. This phenomenon can induce yielding in the superstructure and amplify the acceleration response at the different floors of the building, depending on the impact velocity, gap distance, and moat wall properties (Komodromos 2008; Masroor and Mosqueda 2012). Significant structural damage due to earthquake-induced impacts has also been observed in bridges, especially at expansion joints and abutments, e.g. after the San Fernando earthquake in 1971 (Zheng et al. 2015) and the 1995 Kobe earthquake (Otsuka et al. 1996). Pounding in bridges can cause local damage around the corners of the deck (e.g. spalling of the deck surface), differential settlements on the abutments, permanent vertical opening of the abutments, concentrated damage at bent caps, and even deck collapse (Chouw and Hao 2012; Otsuka et al. 1996). Seismic pounding in nuclear power plants has been also widely investigated. For example, Pellissetti et al. (2017) studied how plastic deformations, due to impacts between fuel assemblies at the space grid levels in a pressure vessel of a nuclear reactor, can affect the reliability of a safety shutdown for increasing seismic intensity levels.

A significant number of studies focused on the evaluation of the critical separation distance to limit the probability of impact between adjacent systems (Barbato and Tubaldi 2013; Lopez-Garcia and Soong 2009; Tubaldi, Barbato, and Ghazizadeh 2012; Tubaldi, Freddi, and Barbato 2016). However, the consequences of pounding were analyzed in fewer investigations, which were often limited to specific structural configurations, fixed excitation levels, and/or prescribed gaps (Anagnostopoulos 1988; Bi, Hao, and Chouw 2010; Desroches and Muthukumar 2002; Pantelides and Ma 1998).

Another issue that has received scarce attention in the literature is the evaluation of the impact forces, despite their importance for assessing the potential damage due to collisions and the effectiveness of different pounding mitigation measures (Jankowski 2006; Vega, Del Rey, and Alarcon 2009; Yaghmaei-Sabegh and Jalali-Milani 2012). The available studies generally considered only the mean response under a reduced representative set of records of the seismic input. Therefore, they neglected the effect of the seismic input uncertainty and record-to-record variability on the response dispersion (Guo, Cui, and Li 2012; Van Mier et al. 1991). Existing parametric studies focused only on a restricted number of engineering demand parameters, namely displacements and/or impact forces, without carrying out additional analyses in terms of acceleration, impact velocity, number of impacts or energy dissipated. However, the analysis of these response parameters can provide an in-depth understanding of the pounding phenomenon and of its effects on the structural performance. For instance, excessive floor accelerations resulting from pounding can lead to damage of acceleration-sensitive non-structural components in buildings. The number of impacts is relevant for systems and components sensitive to damage accumulation.

Based on the existing literature, pounding phenomena can be classified into two classes: (1) pounding between two adjacent flexible structures with out-of-phase vibrations, e.g. adjacent buildings, adjacent spans of bridges, and bridges decks impacting bent caps (Brown and Elshaer 2022); and (2) pounding of a flexible structure impacting a significantly stiffer (ideally rigid) system, e.g. seismically-isolated buildings impacting moat walls (Komodromos et al. 2007), and bridge decks impacting bridge abutments (Hao et al. 2013). In the former case, the most relevant issues are the determination of the probability of impact for a given gap, the calculation of the critical separation distance to achieve a desired reliability, or the estimation of the impact force, as they depend on the relative motion of the two adjacent dynamic systems (Brown and Elshaer 2022). In the latter case, the probability of impact and the critical separation distance are easier to calculate, as they depend on the motion of a single dynamic system. Thus, the most relevant issue becomes the characterization of the impact forces and the corresponding peak accelerations transmitted to the structure, both from a deterministic and a probabilistic viewpoint.

Crozet et al. (2018) carried out a global sensitivity analysis to investigate the most influential parameters (i.e. frequency ratio, mass ratio, and restitution coefficient) for the force and displacement

response of adjacent single-degree-of-freedom (SDOF) systems undergoing pounding when considering multiple constitutive models. The sensitivity indexes were derived for systems with relatively low frequency of vibration, below under 5 Hz, by employing a Kanai-Tajimi model (Kanai 1957; Tajimi 1960) to describe the seismic input. This model is convenient for parametric studies, since it is characterized by only two parameters, but its use may lead to inaccurate results for systems with low vibration frequency (Li, Sun, and Ren 2008). Moreover, this sensitivity study was carried out only for the mean response, obtained considering five seismic inputs to limit computational efforts. The limited number of records did not allow to investigate the sensitivity of the response dispersion. Wu et al. (2019) studied the response of an oscillator impacting against a rigid wall with the aid of dimensional analysis. However, they investigated only the case of harmonic input excitation; therefore, the analysis of this problem under a more realistic description of the seismic input is needed to gain additional insight into the earthquake response of structural systems.

The present paper aims to advance the understanding of the performance of systems undergoing pounding and of the most influential parameters that control it. It focuses on the seismic pounding between a flexible and a rigid structure, which is a condition representative, e.g. of the pounding impact of seismically-isolated structures against moat walls or of bridge decks against lateral abutments. A simplified structural system is considered, which consists of an SDOF linear elastic system surrounded by a rigid wall. The widely employed modified Kelvin – Voigt element is used to simulate the impact (Komodromos et al. 2007), whereas a stochastic model is adopted to describe the uncertainty in the seismic input intensity and characteristics (Atkinson and Silva 2000). More specifically, the performed analyses require a significant number of simulations under records with different intensity and frequency content. Stochastic methods can create a large number of records rapidly, helping to remove potential gaps and biases in empirical data. Jalayer and Beck (2008) provide an in-depth comparison between the two approaches for hazard and risk assessment.

The controlling non-dimensional parameters (representative of both seismic input and structural system) are derived via a dimensional analysis of the problem. A parametric analysis is performed to investigate how the statistics of the various response parameters of interest are affected by the non-dimensional input and system parameters. A probabilistic seismic demand model is derived for the pounding forces, through a nonlinear regression analysis that allows to account explicitly for the effect of the separation gap, the seismic input intensity, the system properties, and the impact stiffness. Finally, a global sensitivity analysis is conducted by computing the Sobol's indexes (Sobol 1993) to investigate the influence of the non-dimensional input parameters on the median response of multiple non-dimensional structural responses of interest.

2. Non-Dimensional Problem Parameters

2.1. Model Description

The system considered in this study is an SDOF model described by three parameters, i.e. the stiffness k, the damping constant c, and the mass m (Fig. 1). The analyzed structural model can be representative of impacts occurring between a base-isolated building with rigid superstructure and the surrounding moat wall, or the pounding between a bridge deck and the lateral abutments. In the first case, the SDOF stiffness k and damping constant c represent the isolation system equivalent linearized stiffness and damping properties, whereas m represents the superstructure mass. The use of equivalent linearized stiffness and damping properties is needed to account for the typically nonlinear behavior of seismic isolation systems. In the second case, k and c represent the substructure stiffness and damping properties, and m represents the deck mass. In addition, the considered SDOF model can provide a simplified approximation of the pounding behavior occurring between the fuel assemblies and the core shroud inside a nuclear reactor. In this last case, k describes the fuel rods stiffness, whereas c describes the damping properties of the spacer grid elements and m the total mass of multiple fuel assemblies. It is noted here that more complex

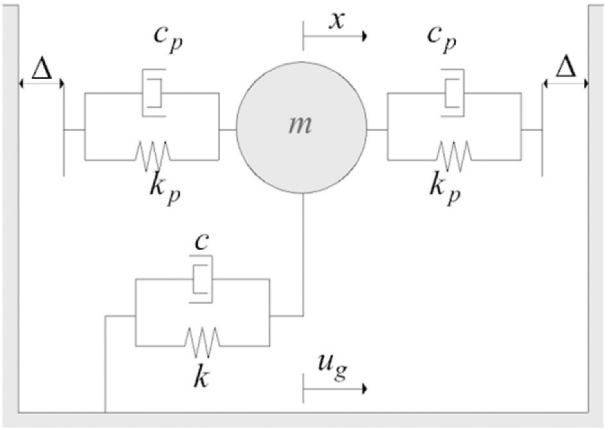

Figure 1. Schematic description of the equivalent mechanical model.

nonlinear and/or multi-degree-of-freedom models could be used to describe the pounding systems. However, these models require the characterization of a larger number of parameters, which complicate the interpretation of the results. These models are necessary to study the structural effects of pounding on the system of interest, which is outside the scope of this work. By contrast, a simple linear elastic SDOF model provides a concise presentation of the problem in terms of few non-dimensional parameters, sufficient to characterize the impact phenomenon and the impact force, which is the focus of this paper.

An appropriate dynamic impact model is needed to describe the pounding phenomenon. Among the several models available in the literature (Banerjee, Chanda, and Das 2017; Goldsmith 1960), this study adopts the one proposed by Komodromos et al. (2007), which represents an improved version of the well-known Kelvin-Voigt model because it avoids the generation of negative impact forces during the separation stage (Goldsmith 1960). Even though other models, e.g. the Hertz-damp models (Jankowski 2005), have been proved to simulate the contact force evolution more accurately in some situations, the Komodromos model is preferred in this study due to its simplicity and convenience for dimensional analysis purposes (Zhai, Jiang, and Chen 2014).

According to the adopted impact model, the temporal evolution of the impact force, $f_p(t)$, during the seismic action can be expressed as follows:

$$f_p(t) = \text{sign}(x) \cdot H(\delta) \cdot \left\langle k_p \cdot \delta(t) + c_p \cdot \dot{\delta}(t) \right\rangle \tag{1}$$

where $_{k_p}$ and $_{c_p}$ are the impact stiffness and damping coefficient, respectively; $\delta(t) = |x(t)| - \Delta$ and $\dot{\delta}(t) = \dot{x}(t) \cdot \text{sign}[x(t)]$ represent the interpenetration depth and relative velocity, respectively, in which sign() denotes the sign function and Δ is the gap between the system and the rigid wall; $\langle \bullet \rangle$ denotes the Macaulay brackets; and $H[]$ represents the Heaviside step function. The impact stiffness k_p depends on several uncertain/unknown quantities, e.g. the geometry of the impact surfaces and the material properties under impact loadings (Anagnostopoulos and Spiliopoulos 1992). In general, in the absence of relevant experimental data, the impact stiffness is assumed proportional to the axial stiffness of the colliding structures (Muthukumar and Desroches 2006). The impact damping coefficient is given by:

$$c_p = 2\xi_p \cdot m \cdot \sqrt{\frac{k_p}{m}} \tag{2}$$

where

$$\xi_p = \frac{-\ln(\varepsilon_r)}{\sqrt{\pi^2 + [\ln(\varepsilon_r)]^2}} \tag{3}$$

in which the parameter ε_r is the coefficient of restitution, which describes the energy dissipation during impact.

2.2. Non-Dimensionalisation of the Equation of Motion

The equation of motion for a SDOF systems subject to seismic excitation and undergoing pounding is:

$$m \cdot \ddot{x}(t) + c \cdot \dot{x}(t) + k \cdot x(t) + f_p(t) = -m \cdot \ddot{u}_g(t) \tag{4}$$

where $f_p(t)$ is given by Eq. (1) and expresses the time-dependent impact force, $\ddot{u}_g(t)$ is the input earthquake ground motion time history, and a superposed dot denotes differentiation with respect to time t. By substituting Eq. (1) into Eq. (4), and dividing the resulting equation by m, the equation of motion of the system becomes:

$$\begin{aligned} &\ddot{x}(t) + 2\xi \cdot \omega \cdot \dot{x}(t) + \omega^2 \cdot x(t) + \\ &+\text{sign}[x(t)] \cdot H(|x(t)| - \Delta) \cdot \left\langle \omega_p^2 \cdot (|x(t)| - \Delta) + 2\xi_p \cdot \omega_p \cdot \text{sign}[x(t)] \cdot \dot{x}(t) \right\rangle = -a_0 \cdot \lambda(t) \end{aligned} \tag{5}$$

where $\omega = \frac{2\pi}{T} = \sqrt{\frac{k}{m}}$, $\xi = \frac{c}{2m \cdot \omega}$, $\omega_p = \sqrt{\frac{k_p}{m}}$, and $\lambda(t)$ denotes the ground motion history scaled by a parameter a_0, with dimension of acceleration and synthetically describing the ground motion intensity.

By introducing the dimensionless time $\tau = t \cdot \omega$ (i.e. time multiplied by the circular frequency of the system, corresponding to 2πtimes the number of cycles of the system) and the dimensionless displacement $\psi(\tau) = \frac{\omega^2 \cdot \bar{x}(\tau)}{a_0}$ (i.e. the ratio of the system's displacement and the seismic input intensity normalized by ω^2), and by dividing Eq. (5) by a_0, the non-dimensional form of the equation of motion is obtained as:

$$\begin{aligned} &\psi''(\tau) + 2\xi \cdot \psi'(\tau) + \psi(\tau) + \\ &+ \text{sign}[\psi(\tau)] \cdot H(1 - \alpha(\tau)) \cdot \left\langle \Pi_{\omega_p}^2 \cdot [|\psi(\tau)| - \Pi_\Delta] + 2\xi_p \Pi_{\omega_p} \cdot \text{sign}[\psi(\tau)] \cdot \psi'(\tau) \right\rangle = -\bar{\lambda}(\tau) \end{aligned} \tag{6}$$

where $\Pi_{\omega_p} = \frac{\omega_p}{\omega} = \sqrt{\frac{k_p}{k}}$ (i.e. the dimensionless ratio between the stiffness of the pounding element and the overall stiffness of the structure), $\alpha(\tau) = \frac{\Delta}{|\bar{x}(\tau)|}$ (i.e. the ratio between the separation gap and the system displacement response), and $\Pi_\Delta = \frac{\omega^2 \Delta}{a_0}$ denotes the dimensionless gap (Vega, Del Rey, and Alarcon 2009), which is given by the ratio between the reference gap distance and the seismic input intensity normalized by ω^2 (similar to the non-dimensional displacement). The quote symbol $\bullet'$ denotes differentiation with respect to the dimensionless time τ, and the overlined quantities $\bar{x}(\tau)$ and $\bar{\lambda}(\tau)$ denote the new functional expressions of the corresponding quantities $x(t)$ and $\lambda(t)$without overline, respectively, when dimensionless time is used.

It is noteworthy that the dimensionless displacement and velocity responses (ψ and ψ'), as well as their derived quantities (e.g. impact forces), depend also on the vibration period of the system through $\bar{\lambda}(\tau)$. In fact, by changing T, also the shape of $\bar{\lambda}(\tau)$ changes for any given seismic record. This implicit dependence of the dimensionless response on T has been explained in other studies carrying out the non-dimensional analysis of similar systems (Tubaldi, Freddi, and Barbato 2016). Thus, the system performance is controlled by the system's natural period T and the following non-dimensional parameters: $\xi, \Pi_{\omega_p}, \xi_p, \Pi_\Delta$. Typical values of ξ for ordinary structures are in the range between 2% and 5% (see e.g. Bernal et al. 2015), whereas for isolated system are in the range between 15% and 30%. A wide range of Π_{ω_p} values have been employed in the literature, as different authors have proposed different approaches for the definition of this parameter. For example, Crozet et al. (2018)

recommended Π_{ω_p} values higher than 100, in order to ensure that the penetration depth during the impact is negligible. However, existing studies (e.g. Crozet et al. 2018; Wu et al. 2019) have shown that the impact stiffness mainly affects the penetration displacements and peak accelerations, whereas other response quantities of interest are not very sensitive to this parameter.

The coefficient of restitution ε_r (and thus ξ_p) can also assume different values in the range between 0 (perfectly plastic impact) and 1 (perfectly elastic impact), depending on the problem considered, although in many previous studies, it has been simply assumed as fixed (e.g. it was assumed equal to 0.7 in Komodromos et al. 2007). The values that can be assumed by the normalized gap Π_Δ depend on the choice of the intensity measure a_0. For example, if the pseudo-spectral acceleration $S_a(T,\xi)$ calculated at the fundamental period of the system for the damping ratio ξ is considered, Π_Δ can be interpreted as the ratio between the gap and the maximum displacement demand in the system when its displacement is not constrained by adjacent structures. Thus, for values of Π_Δ larger than or equal to 1 pounding does not occur.

The next section presents the results of an extensive parametric study that was performed to investigate the influence of the identified non-dimensional input parameters on the performance of the system. In particular, the following dimensionless output parameters are considered: (1) non-dimensional impact force Π_{f_p}, (2) non-dimensional absolute acceleration Π_a, (3) numbers of impacts per seismic event n_p, (4) non-dimensional impact dissipated energy Π_E, and (5) non-dimensional impact velocity Π_v.

The quantities Π_a and Π_v are computed by normalizing the maximum absolute acceleration and impact velocity measured during the entire earthquake time history with respect to a_0 and $\omega \cdot a_0$, respectively, i.e. $\Pi_a = \frac{\max_t\left|\ddot{x}(t)+\ddot{x}_g(t)\right|}{a_0}$ and $\Pi_v = \frac{\max_t|\dot{x}(t)|}{m\cdot a_0}$. Thus, Π_a and Π_v represent the amplification factor of the absolute accelerations and velocities due to pounding. Π_{f_p} is obtained by dividing the maximum pounding force during the seismic event by $m \cdot a_0$, i.e. $\Pi_{f_p} = \frac{\max_t\left|f_p(t)\right|}{m\cdot a_0}$; whereas the energy dissipated through the impacts during a given seismic event is computed as:

$$\Pi_E = \frac{\sum_j E_{pj}}{E_i} = \frac{\sum_j \int_{t_{ji}}^{t_{je}} c_p \cdot \dot{\delta}(t) \cdot \mathrm{d}\delta(t)}{-\int_0^{t_f} m \cdot \dot{x}(t) \cdot \ddot{u}_g(t) \cdot \mathrm{d}t} \tag{7}$$

where E_{pj} represents the energy dissipated by the j-th impact in the time interval $[t_{ji},t_{je}]$ during which $\delta(t) \geq 0$; and E_i represents the relative input energy introduced into the system by the seismic event during its entire duration t_f.

In order to illustrate the benefits of the non-dimensional formulation, two different systems are analyzed, which share the same fundamental period ($T = 0.45s$), damping ratio ($\xi = 0.05$), Π_{ω_p} values, ξ_p values, and Π_Δ values, but are characterized by different gap ($\Delta_2 = 2\Delta_1$) and are subjected to a seismic input with different intensity values ($a_{02} = 2a_{01}$). Figure 2 shows that the responses of the two systems are identical if the non-dimensional parameters are considered, thus demonstrating the benefits of the non-dimensional formulation in terms of reduction of parameters to be varied in the parametric study.

3. Parametric Study: Results and Discussion

In order to perform the proposed parametric study, a set of 100 ground motion samples is generated by sampling the random variables representing the earthquake input model described in Appendix A (Atkinson and Silva 2000). In particular, Latin Hypercube Sampling (LHS) (Mckay, Beckman, and Conover 1979) is used to explore efficiently the domain of variation of the input parameters. The adopted seismic model is a point-source model, in which each ground motion sample is characterized by a different intensity, frequency content, and duration. Alternative seismic models or suites of historical ground motion records could also be used to

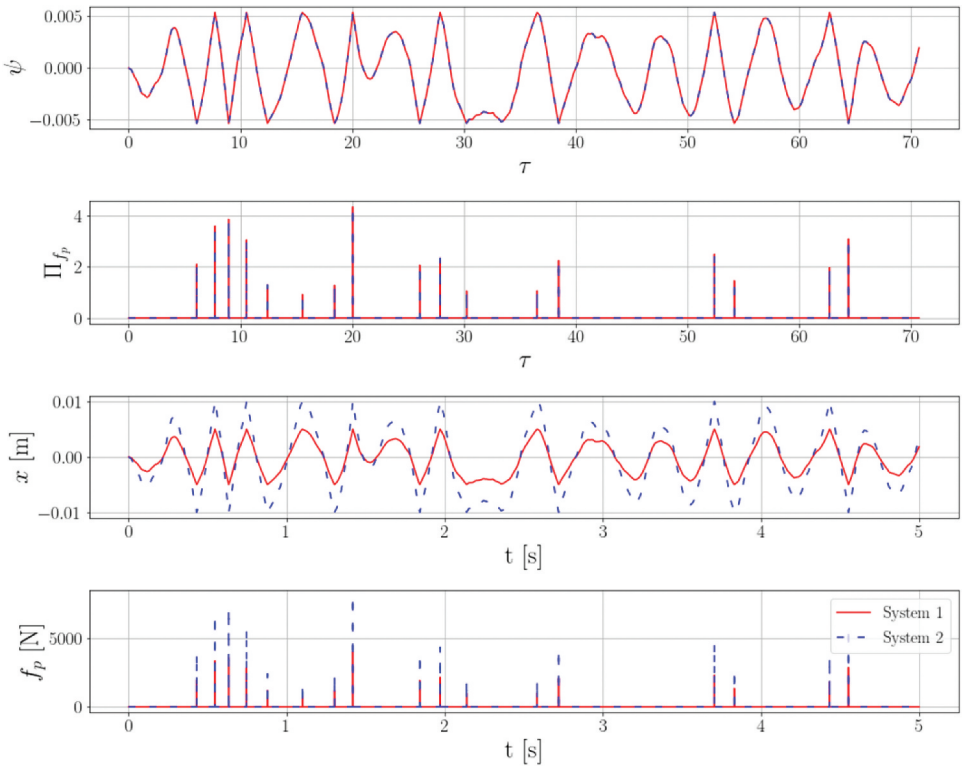

Figure 2. Comparison of displacement and impact force over time for dimensional and non-dimensional systems with proportional gap Δ and seismic intensity a_0.

characterize the seismic demand of the system under investigation without affecting the methodology presented in this study. The effects of record intensity are considered indirectly via non-dimensionalisation, since the earthquake input and the response parameters of interest are normalized by dividing them by a_0. The effects of record-to-record variability are considered by computing the median and the dispersion (i.e. lognormal standard deviation) of the values of the monitored response parameters obtained for the 100 ground motion samples. The intensity measure a_0 adopted in this work is $S_a(T, \xi)$.

Table 1 reports the values of the input parameters $\mathbf{\Gamma} = [\Pi_\Delta, \Pi_{\omega_p}, T]$ considered for the parametric study. The values used for Π_{ω_p} and T cover the realistic ranges that these two parameters can assume for practical engineering applications. The effects of the dimensionless gap Π_Δ are considered only for values smaller than one, which correspond to cases when pounding occurs. It is noted here that changes in the dimensionless gap can be interpreted in two ways: (1) as changes in the gap for a fixed ground motion intensity, which is of interest when determining the critical separation distance for a given design earthquake; or (2) as scaling of the ground motion for a given gap, which is of interest, e.g. when performing an incremental dynamic analysis for a given system. All analyses assume constant values for the damping factor ($\xi = 0.05$, which is typically recommended by seismic design codes) and coefficient of restitution

Table 1. Input values used for the parametric study.

Parameters	Values								
Π_Δ	0.1	0.2	0.5	0.67	0.71	0.77	0.83	0.91	0.99
Π_{ω_p}	5	10	50	100	500				
T [s]	0.1	0.5	1	2	4				

($\varepsilon_r = 0.65$). The choice of employing only one value of ε_r (and thus a single value for ξ_p) is motivated by the fact that this parameter does not significantly affect the response, as observed in other studies (Crozet et al. 2018) and confirmed by the global sensitivity analysis whose results are presented in the final section of this paper. For each combination of the input parameter values, the corresponding median output vector, $\Phi = [\widehat{\Pi}_{f_p}, \widehat{\Pi}_a, \widehat{\Pi}_v, \widehat{\Pi}_E, \widehat{n}_p]$, and dispersion, $\beta = [\beta_{f_p}, \beta_a, \beta_v, \beta_E, \beta_n]$, are computed. The Matlab function ODE23, based on the Bogacki – Shampine method (Bogacki and Shampine 1989), is employed here to solve the equation of motion by using an adaptive time-step.

Due to space constraint, only select subsets of the parametric study's results are illustrated in Figs. 3–8 (i.e. median values for all considered output parameters and dispersion of the dimensionless pounding force). In general, it is observed that the median values of the amplification factors $\widehat{\Pi}_{f_p}$, $\widehat{\Pi}_a$, and $\widehat{\Pi}_v$ show a very similar trend of variation with T and Π_Δ (Figs. 3–5). The similarity between $\widehat{\Pi}_{f_p}$ and $\widehat{\Pi}_a$ is expected, because these two parameters coincide for systems without damping. The values of $\widehat{\Pi}_{f_p}$, $\widehat{\Pi}_a$, and $\widehat{\Pi}_v$ increase for increasing T, while their variation with Π_Δ depends on the value assumed by Π_{ω_p}. For $\Pi_{\omega_p} > 10$, all three amplification factors increase with Π_Δ increasing from 0 to approximately 0.5 and decrease with Π_Δ increasing from approximately 0.5 to 1. A similar trend is observed also for $\Pi_{\omega_p} \leq 10$ and low T values (depending on the Π_{ω_p} values), whereas for $\Pi_{\omega_p} \leq 10$ and higher T values, the three amplification factors decrease for increasing Π_Δ. The maximum values of the amplification factors $\widehat{\Pi}_{f_p}$ and $\widehat{\Pi}_a$ increase almost linearly with Π_{ω_p}, and can assume very large values, as high as 1750 and 1250, respectively, in the case of very large ratios of impact stiffness and system stiffness $\left(\Pi_{\omega_p} \geq 500\right)$. The amplification factor $\widehat{\Pi}_v$ is not significantly affected by Π_{ω_p}.

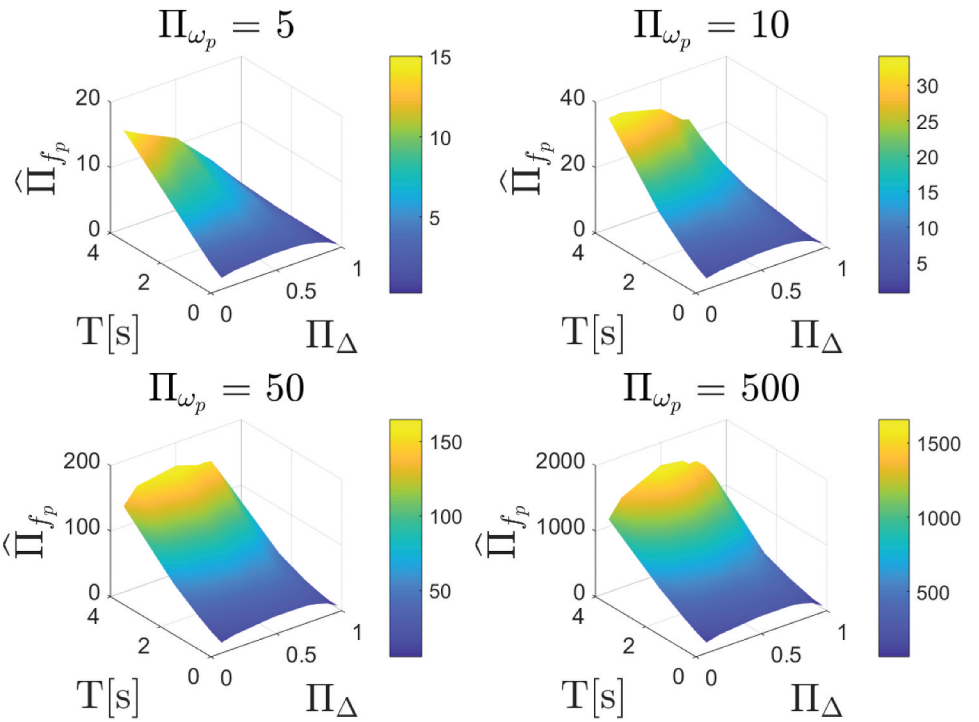

Figure 3. Median dimensionless pounding force vs. T, $\prod_\Delta$ and Π_{ω_p}.

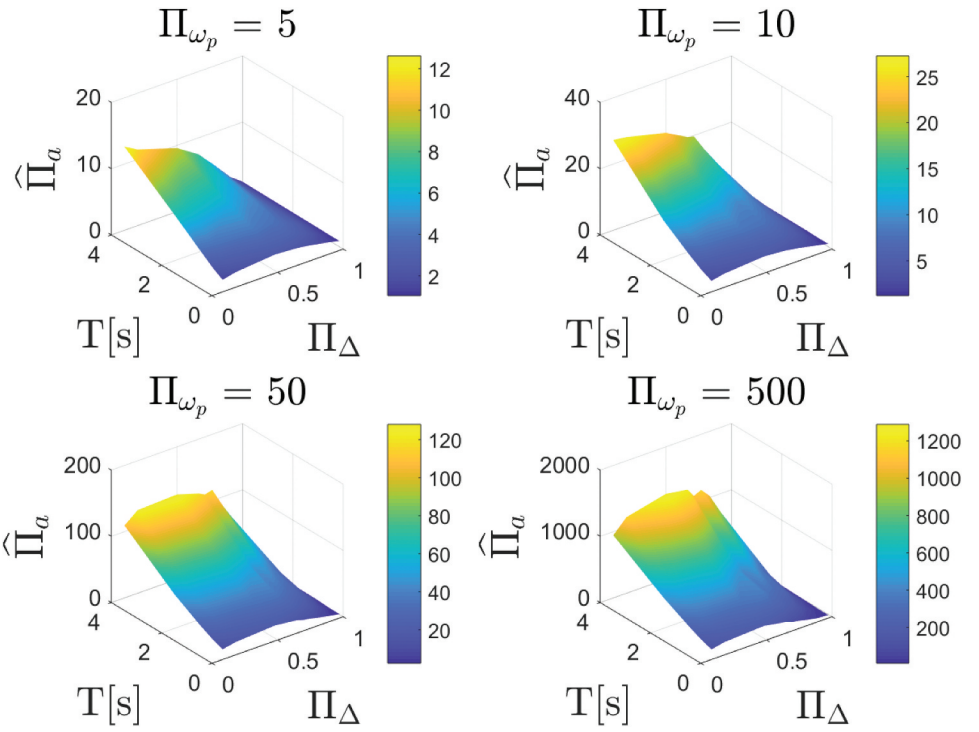

Figure 4. Median dimensionless maximum acceleration vs. T, $\prod_\Delta$ and Π_{ω_p}.

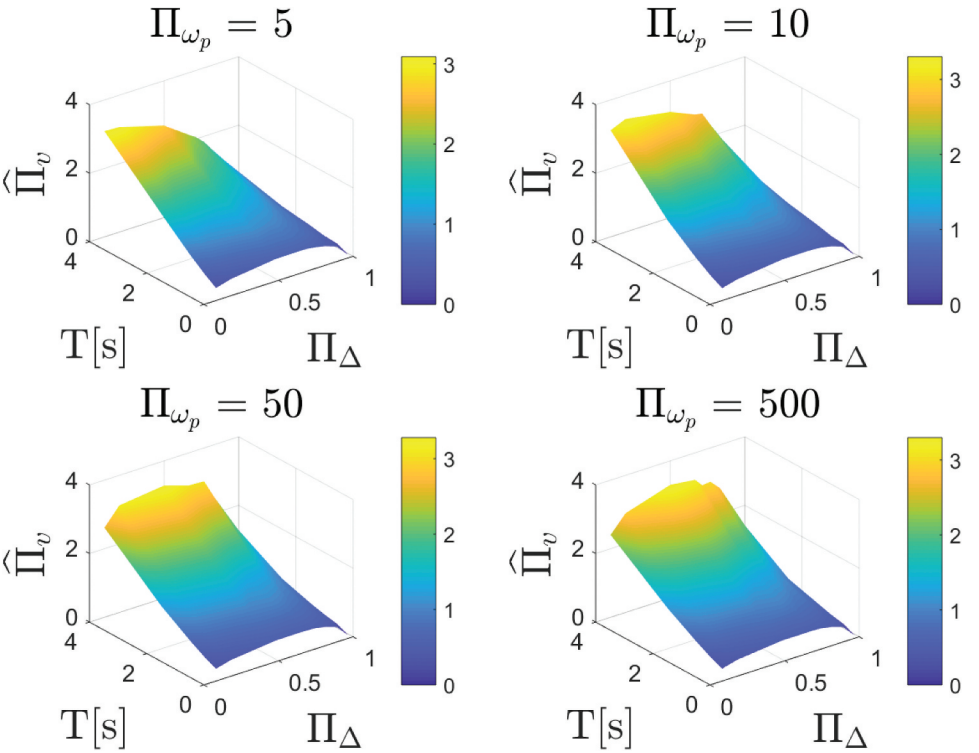

Figure 5. Median dimensionless maximum impact velocity vs. T, $\prod_\Delta$ and Π_{ω_p}.

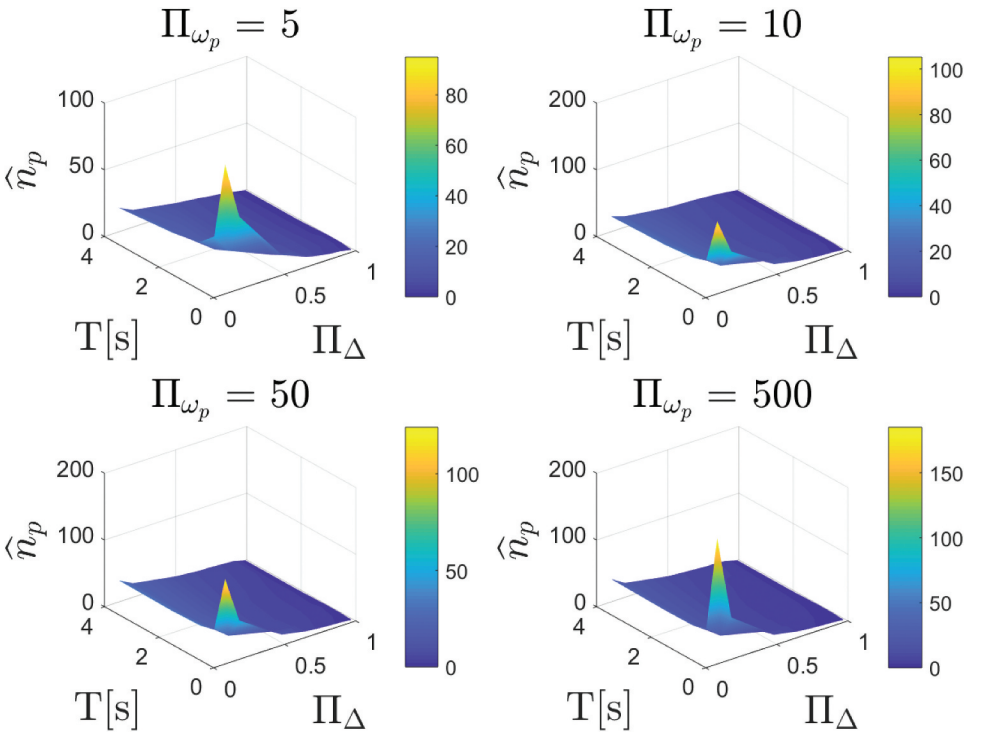

Figure 6. Median number of impacts vs. T, $\prod_\Delta$ and Π_{ω_p}.

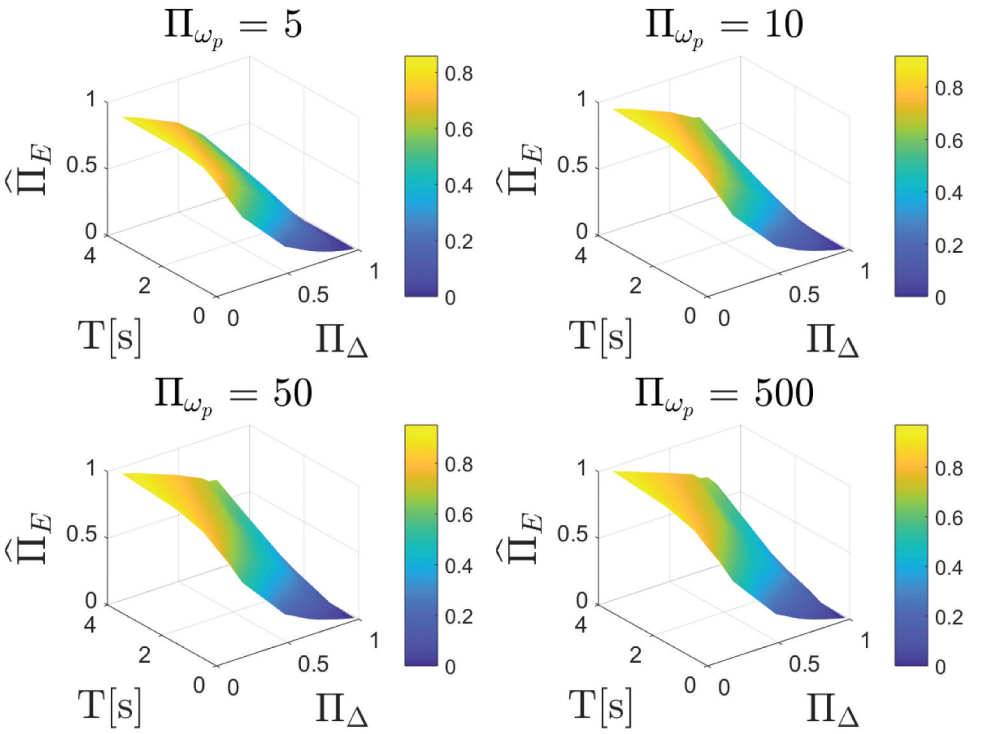

Figure 7. Median dimensionless dissipated energy vs. T, $\prod_\Delta$ and Π_{ω_p}.

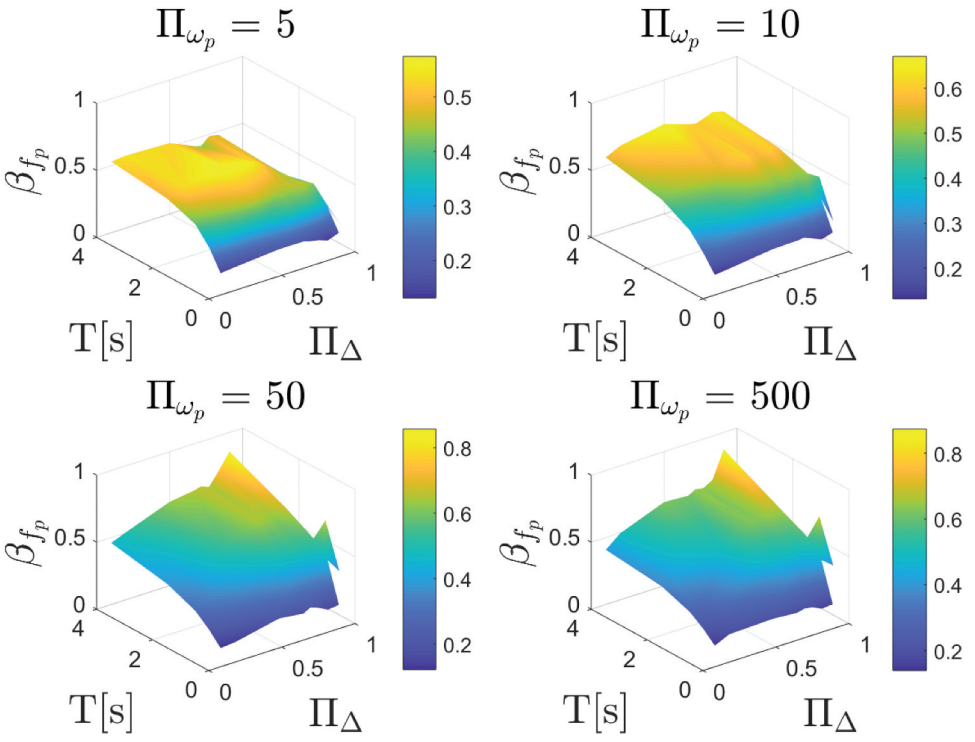

Figure 8. Logarithmic standard deviation of the dimensionless pounding forces vs. T, Π_Δ and Π_{ω_p}.

The median value of the number of impacts, $\widehat{n}_p$, is generally little sensitive to changes in Π_Δ, Π_{ω_p}, and T, except for small values of Π_Δ(< 0.3) and T (<0.4s), for which it increases significantly (Fig. 6). The median value of the dimensionless dissipated energy, $\widehat{\Pi}_E$, increases for decreasing Π_Δ and increasing T, whereas its sensitivity to Π_{ω_p} is generally small (Fig. 6).

The parameter β_{f_p}, which describes the dispersion of the normalized impact forces, increases significantly for increasing values of the period T, changes with Π_Δ without following a clear trend, and is not very sensitive to Π_{ω_p}. The maximum values are generally attained for high values of T (>2s) and Π_Δ (>0.5), with values of the order of 0.6 to 1. The other dispersion parameters (β_a,β_v,β_{n_p}, and β_E) are not graphically reported here due to space limitations, but present similar trends as those shown by β_{f_p}. They are mainly sensitive to Π_Δ, with maximum values reached for $\Pi_\Delta > 0.7$, whereas only β_a results to be more sensitive to Π_{ω_p}, with maximum values achieved for $\Pi_{\omega_p} > 50$.

4. Probabilistic Seismic Demand Model for Pounding Forces

The results of the previous parametric study can be used to build a probabilistic seismic demand model for estimating the pounding forces corresponding to the system in Fig. 1. The model is developed in non-dimensional form through nonlinear regression, assuming $\mathbf{\Gamma} = [\Pi_\Delta, \Pi_{\omega_p}, T]$ and $\Omega = [\widehat{\Pi}_{f_p}, \beta_{f_p}]$ as the input and output vectors, respectively.

The predicted median dimensionless impact force $\widehat{\Pi}_{f_p}$ is given by the following equation:

$$\hat{\Pi}_{f_p}(\Gamma) = I \cdot \left[e^{-b(1/\Pi_\Delta - 1)} - e^{-c(1/\Pi_\Delta - 1)}\right](T) \cdot \left(\Pi_{\omega_p}\right) \cdot \varepsilon \tag{8}$$

Table 2. Regression's coefficients and R^2 values for the pounding force statistics' regression models.

	R^2	a	b	c	g_1	g_2	p_1	p_2
$\hat{\Pi}_{f_p}(\Pi_\Delta, \Pi_{\omega_p}, T)$	0.989	19.800	0.039	7.205	0.283	0.615	−0.037	0.053
	R^2	h_1	h_2	q_1	q_2	w_1	w_2	w_3
$\beta_{f_p}(\Pi_\Delta, \Pi_{\omega_p}, T)$	0.841	−0.015	0.001	0.523	0.001	−25.118	−41.458	6.001

where ε is the error due to the lack of fit, I represents an indicator function equal to 1 when impacts occur (i.e. for $0 < \Pi_\Delta < 1$) and 0 otherwise (i.e. for $\Pi_\Delta \geq 1$), $g(T) = g_1 \cdot T + g_2$ and $p(\Pi_{\omega_p}) = p_1 \cdot \Pi_{\omega_p} + p_2$ are linear functions depending on T and Π_{ω_p}, respectively.

Similarly, the following regression model is proposed to estimate β_{f_p} as a function of $\boldsymbol{\Gamma}$:

$$\beta_{f_p}(\boldsymbol{\Gamma}) = h(\Pi_\Delta) \cdot q(\Pi_{\omega_p}) \cdot w(T) \cdot \varepsilon_\beta \tag{9}$$

where $h(\Pi_\Delta) = h_1 \cdot \Pi_\Delta + h_2$ and $q(\Pi_{\omega_p}) = q_1 \cdot \Pi_{\omega_p} + q_2$ are linear functions depending on Π_Δ and Π_{ω_p}, respectively, while $w(T) = w_1 \cdot T^2 + w_2 \cdot T + w_3$ is a quadratic function of T, and ε_β is the error due to the lack of fit.

The constant coefficients in Eqs. (8) and (9) are identified by minimizing the sum of squares of all the residuals through the Levenberg-Marquardt optimization algorithm (Moré 1978). The fitted parameters of both regression models are reported in Table 2. The proposed model represents an improvement of the model previously proposed in Altieri et al. (2018), based on a larger seismic dataset (100 samples) that results in a more accurate and robust regression, especially for the β_{f_p} parameter.

Figures 9 and 10 compare the values of $\hat{\Pi}_{f_p}$ and β_{f_p} obtained from the parametric study (i.e. direct simulation of the system response) and the regression model for $\Pi_{\omega_p} = 50$ and $\Pi_{\omega_p} = 100$. A good

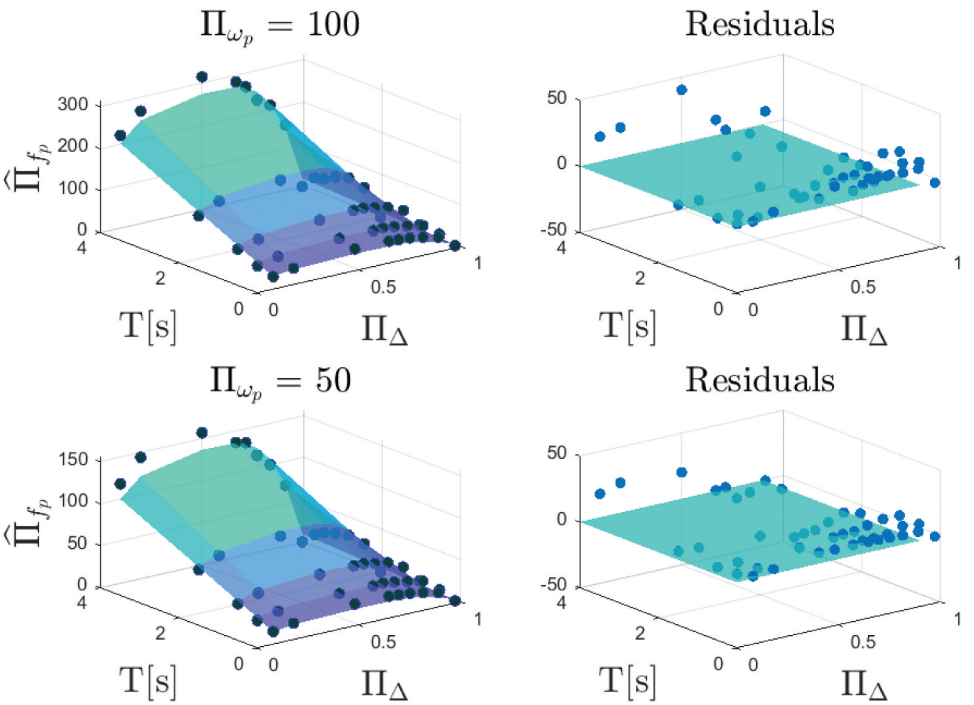

Figure 9. Comparison between $\hat{\Pi}_{f_p}$ estimates from parametric study and regression model for Π_{ω_p}=50 and Π_{ω_p}=100.

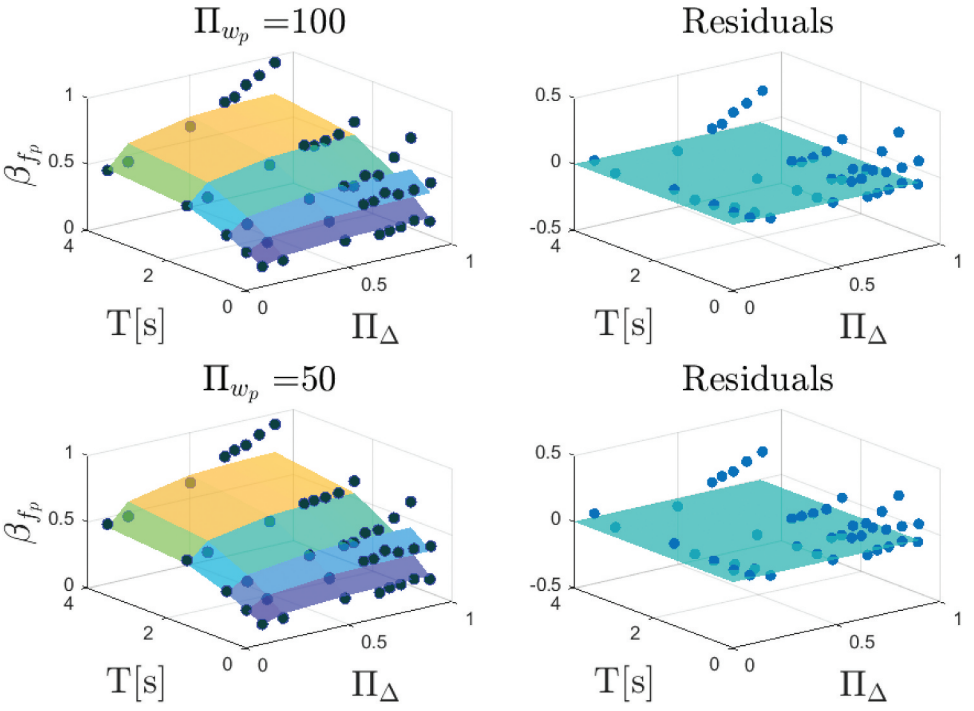

Figure 10. Comparison between β_{f_p} estimates from parametric study and regression model for Π_{ω_p}=50 and Π_{ω_p}=100.

agreement is observed for the values of $\hat{\Pi}_{f_p}$ given by Eqs. (8) with respect to all investigated parameter combinations, as demonstrated by the high value of the coefficient of determination $R^2 = 0.989$. A similarly good agreement is also observed between the estimates of the dispersion β_{f_p} obtained via the parametric study and the regression model corresponding to Eqs. (9) with $R^2 = 0.841$.

It is noteworthy that using the proposed regression formulae, the estimates of the median value of the pounding force and of its dispersion can be easily obtained for each desired intensity level. The median pounding force for an intensity level $IM = im$ is given as $\hat{f}_p = m \cdot im \cdot \hat{\Pi}_{f_p}$, whereas the dispersion coincides with β_{f_p}. By introducing an assumption on the distribution of the pounding force f_p, e.g. assuming lognormality of (Baker 2015), it is also possible to estimate the pounding force's conditional probability of exceedance $P(f_p \geq f_{p_i} | IM = im)$ for given $IM = im$. However, the development and evaluation of this model is outside the scope of this paper.

5. Global Sensitivity Analysis

A global sensitivity analysis (Patelli, Pradlwarter, and Schuëller 2010) is carried out to further investigate how the various input non-dimensional parameters (i.e. Π_Δ, Π_{ω_p}, and the coefficient of restitution ε_r) affect the performance parameters of interest. The first and total sensitivity indexes are computed with respect to several response parameters in addition to the impact forces. A similar analysis was carried out in Crozet et al. (2018), but considering a different structural system and a limited set of ground motions for describing record-to-record variability effects. In this study, the seismic dataset employed is extended to $n_a = 10$ accelerograms, in order to obtain more accurate estimates of the response.

The median values of the response parameters of interest are considered as output variables in the global sensitivity analysis. The sensitivity indices are computed for different values of the vibration period T. All input parameters are described by uniform distributions, with upper and lower bounds

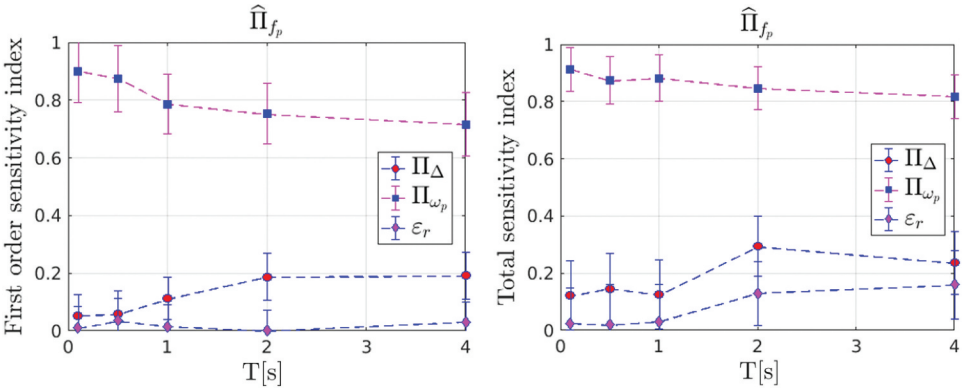

Figure 11. First (left) and total (right) sensitivity indexes with associated standard deviations for.

equal to 0.1 and 0.99, respectively, for Π_Δ; equal to 5 and 500, respectively, for Π_{ω_p}; and equal to 0 and 1, respectively, for ε_r.

The algorithm presented by Saltelli et al. (2008) is adopted here to compute the first and total Sobol' sensitivity indexes. The global sensitivity analysis is based on a decomposition of the variance of each output parameter resulting from variations of the input parameters in the range of interest. A total of $(N_{inp}+2)\cdot n$ structural analyses are required for each structural system, where $N_{inp}=3$ represents the number of inputs, and n indicates the number of input parameter samples employed to compute the indexes for each input. LHS is employed for the samples generation, with $n=1500$. The five values of T $(n_T=5)$ listed in Table 1 are considered for the sensitivity analysis, for a total of $(N_{inp}+2)\cdot n\cdot n_a\cdot n_T=375,000$ structural samples. The OpenCossan Matlab toolbox (Patelli 2016; Patelli et al. 2018) is used to perform the global sensitivity analysis.

The results of the global sensitivity analysis are qualitatively consistent with those of the parametric study. They confirm that the impact forces (Fig. 11) and the maximum accelerations (Fig. 12) are influenced primarily by the frequency ratio Π_{ω_p}, with only a minor dependency on Π_Δ. This result highlights the importance of accurate estimates of the pounding impact stiffness on the estimation of the impact forces and maximum accelerations produces by seismic pounding. The sensitivity indexes associated with the impact velocity (Fig. 13), the number of impacts (Fig. 14), and the energy dissipated (Fig. 15), clearly identify the dimensionless gap Π_Δ as the most important input parameter, whereas the effect of Π_{ω_p} is almost negligible. As already observed in the literature for a different structural system

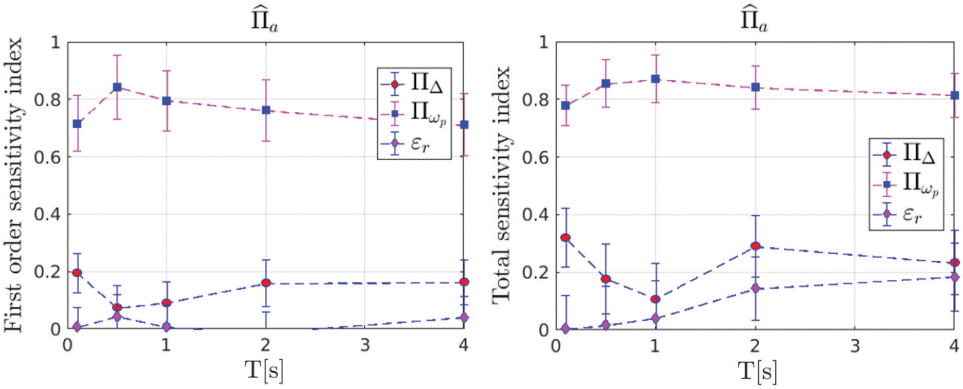

Figure 12. First (left) and total (right) sensitivity indexes with associated standard deviations for $\widehat{\Pi}_a$.

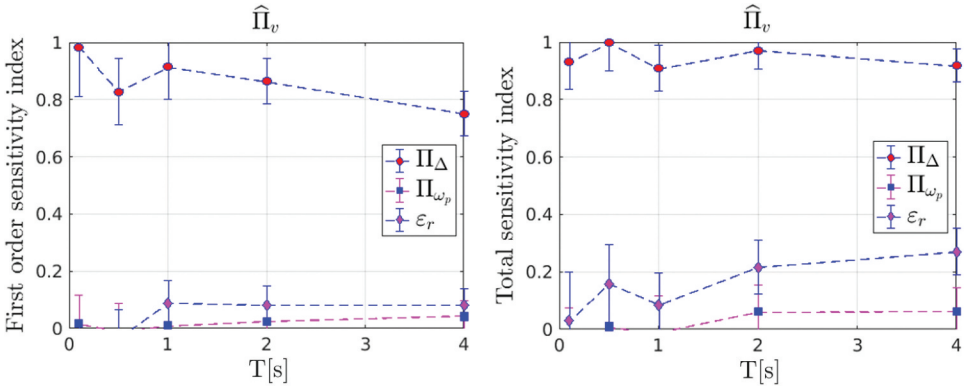

Figure 13. First (left) and total (right) sensitivity indexes with associated standard deviations for $\widehat{\Pi}_v$.

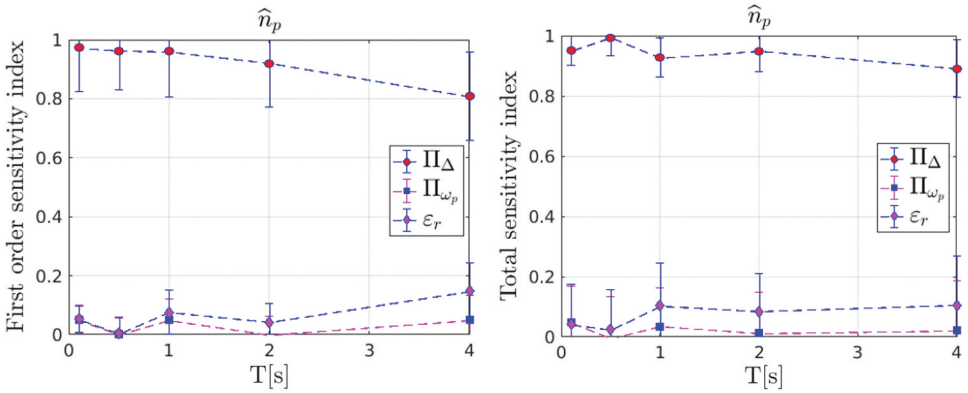

Figure 14. First (left) and total (right) sensitivity indexes with associated standard deviations for $\widehat{n}_p$.

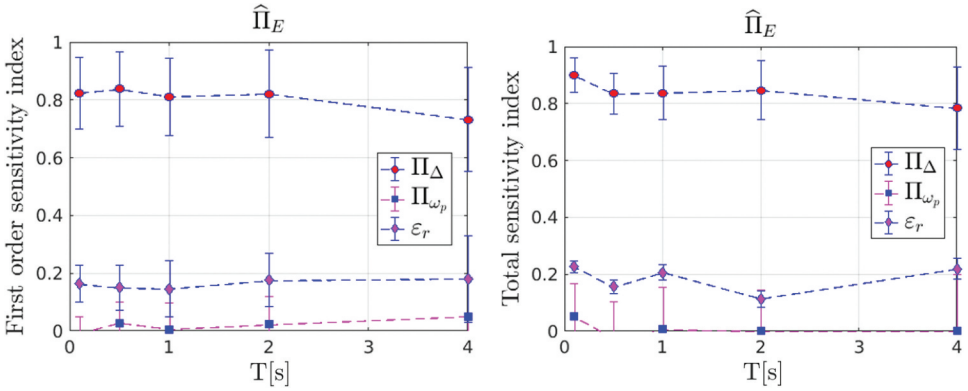

Figure 15. First (left) and total (right) sensitivity indexes with associated standard deviations for $\widehat{\Pi}_E$.

(Crozet et al. 2018), the coefficient of restitution, ε_r, has a low influence on all the considered outputs, with the exception of the median of the normalized dissipated energy $\widehat{\Pi}_E$. This result justifies the consideration of a constant value of ε_r in the parametric study presented in the previous section. It also suggests that pounding mitigation measures aimed at reducing the impact coefficient of restitution can

be expected to be less effective than those aimed at reducing the impact stiffness. The influence of the vibration period T on the sensitivity indexes is also very small. Finally, the total indexes are comparable with the first order indexes, which indicates that input parameters' interaction has a small effect on the output variance.

6. Conclusions

This paper provides a comprehensive analysis of the probabilistic performance of single-degree-of-freedom systems subjected to seismic actions and undergoing impacts with a rigid wall. The presented simplified system can represent different structural configurations commonly encountered in engineering practice. The analysis is based on a rigorous non-dimensionalization of the equations of motion, in conjunction with the Komodromos dynamic impact model and a synthetic seismic ground motion model for stochastic sampling of the input time histories.

An extensive parametric study conducted on the non-dimensional model shows that seismic pounding can result in significant amplifications of the response of the system in terms of absolute accelerations and impact forces. The findings emphasize the crucial role of impact stiffness in governing the amplifications induced by seismic pounding, as these amplifications significantly increase for increasing values of the normalized impact stiffness. By contract, the influence of the system period on these amplifications is comparatively less pronounced, i.e. relatively smaller amplifications of the pounding forces and absolute accelerations are observed for increasing values of the system period. The variation of impact forces and accelerations with the dimensionless gap unveils a more intricate behavior, driven by the natural period of the system and the impact stiffness. The coefficient of restitution is observed to have a minor impact on the estimated responses, suggesting its limited influence in the context of seismic pounding. It is also observed that impact velocity, number of impacts, and impact dissipated energy have a generally small sensitivity to the impact stiffness. The dispersion parameter for the impact forces significantly increases for increasing natural period, changes with the separation gap without following a clear trend, and is not very sensitive to the impact stiffness. Similar trends are observed for the dispersion parameters of other response quantities. It is concluded that the impact stiffness is a key model parameter that requires an accurate estimate and/or calibration to describe the seismic pounding phenomenon, and that pounding mitigation measures should seek to reduce the impact stiffness rather than the coefficient of restitution. However, the limited influence of the coefficient of restitution needs to be further investigated in order to assess if this conclusion remains valid also for more complex structural systems and/or different material properties.

The parametric study results are used to develop a regression model for the estimation of the median value of the pounding force and of its dispersion corresponding to different input parameter combinations. Moreover, considering non-dimensional parameters in the development of the regression model allows to obtain estimates of the response statistics at any intensity levels, based on a single expression for the median normalized force and its dispersion. This model can be useful for estimating the unconditional risk of exceedance of the pounding forces in the system due to any potential threatening earthquake.

The results of the global sensitivity analysis are qualitatively consistent with those of the parametric study. In particular, impact forces and maximum absolute accelerations are influenced primarily by the impact stiffness and present a small dependency on the separation gap. By contrast, the impact velocity, the number of impacts, and the dissipated energy depend mostly on the dimensionless gap and are minimally affected by the impact stiffness. The coefficient of restitution has always a small influence on all response quantities, except for the median of the normalized dissipated energy.

Further research in this area could focus on exploring additional factors that may influence the pounding phenomenon, such as soil-structure interaction, non-linear behavior, and mitigation strategies, to enhance structural resilience and safety.

Disclosure Statement

No potential conflict of interest was reported by the author(s).

Funding

The work was supported by the EPSRC [EP/L015927/1]; EPSRC centre for doctoral training in Risk and Uncertainty [EP/L015927/1].

ORCID

Domenico Altieri http://orcid.org/0000-0002-9441-388X
Enrico Tubaldi http://orcid.org/0000-0001-8565-8917
Michele Barbato http://orcid.org/0000-0003-0484-8191
Edoardo Patelli http://orcid.org/0000-0002-5007-7247

Data Availability Statement

The data that support the findings of this study are available from the corresponding author, E.P., upon reasonable request.

References

Altieri, D., E. Patelli, H. Kessler, M. Pellissetti, and E. Patelli. 2020. "Machine Learning Approaches for Performance Assessment of Nuclear Fuel Assemblies Subject to Seismic-Induced Impacts." *ASCE-ASME Journal of Risk and Uncertainty: Part B* 6 (4). https://doi.org/10.1115/1.4046926.

Altieri, D., E. Tubaldi, and E. Patelli 2018. "Probabilistic Seismic Assessment of Pounding Forces." In *16th European Conference on Earthquake Engineering*. Thessaloniki. http://papers.16ecee.org/files/Paper%20AD.pdf.

Anagnostopoulos, S. A. 1988. "Pounding of Buildings in Series During Earthquakes." *Earthquake Engineering & Structural Dynamics* 16 (3): 443–456. https://doi.org/10.1002/eqe.4290160311.

Anagnostopoulos, S. A., and K. V. Spiliopoulos. 1992. "An Investigation of Earthquake Induced Pounding Between Adjacent Buildings." *Earthquake Engineering & Structural Dynamics* 21 (4): 289–302. https://doi.org/10.1002/eqe.4290210402.

Atkinson, G. M., and W. Silva. 2000. "Stochastic Modeling of California Ground Motions." *Bulletin of the Seismological Society of America* 90 (2): 255–274. https://doi.org/10.1785/0119990064.

Au, S., and J. Beck. 2003. "Subset Simulation and Its Application to Seismic Risk Based on Dynamic Analysis." *Journal of Engineering Mechanics* 129 (8): 901–917. https://doi.org/10.1061/(ASCE)0733-9399(2003)129:8(901).

Baker, J. W. 2015. "Efficient Analytical Fragility Function Fitting Using Dynamic Structural Analysis." *Earthquake Spectra* 31 (1): 579–599. https://doi.org/10.1193/021113EQS025M.

Banerjee, A., A. Chanda, and R. Das. 2017. "Historical Origin and Recent Development on Normal Directional Impact Models for Rigid Body Contact Simulation: A Critical Review." *Archives of Computational Methods in Engineering* 24 (2): 397–422. https://doi.org/10.1007/s11831-016-9164-5.

Barbato, M., and E. Tubaldi. 2013. "A Probabilistic Performance-Based Approach for Mitigating the Seismic Pounding Risk Between Adjacent Buildings." *Earthquake Engineering & Structural Dynamics* 42 (8): 1203–1219. https://doi.org/10.1002/eqe.2267.

Bernal, D., M. Döhler, S. M. Kojidi, K. Kwan, and Y. Liu. 2015. "First Mode Damping Ratios for Buildings." *Earthquake Spectra* 31 (1): 367–381. https://doi.org/10.1193/101812EQS311M.

Bertero, V. V. 1987. "Observations on Structural Pounding." In *The Mexico Earthquakes, 1985: Factors Involved and Lessons Learned*, 264–278. Mexico: ASCE.

Bi, K., H. Hao, and N. Chouw. 2010. "Required Separation Distance Between Decks and at Abutments of a Bridge Crossing a Canyon Site to Avoid Seismic Pounding." *Earthquake Engineering & Structural Dynamics* 39 (3): 303–323. https://doi.org/10.1002/eqe.943.

Bogacki, P., and L. F. Shampine. 1989. "A 3 (2) Pair of Runge-Kutta Formulas." *Applied Mathematics Letters* 2 (4): 321–325. https://doi.org/10.1016/0893-9659(89)90079-7.

Boore, D. M. 2003. "Simulation of Ground Motion Using the Stochastic Method." *Pure and Applied Geophysics* 160 (3): 635–676. https://doi.org/10.1007/PL00012553.

Brown, T., and A. Elshaer. 2022. "Pounding of Structures at Proximity: A State-Of-The-Art Review." *Journal of Building Engineering* 48:103991. https://doi.org/10.1016/j.jobe.2022.103991.

Chouw, N., and H. Hao. 2012. "Pounding Damage to Buildings and Bridges in the 22 February 2011 Christchurch Earthquake." *International Journal of Protective Structures* 3:123–139. https://doi.org/10.1260/2041-4196.3.2.123.

Crozet, V., I. Politopoulos, M. Yang, J. M. Martinez, and S. Erlicher. 2018. "Sensitivity Analysis of Pounding Between Adjacent Structures." *Earthquake Engineering & Structural Dynamics* 47 (1): 219–235. https://doi.org/10.1002/eqe.2949.

Desroches, R., and S. Muthukumar. 2002. "Effect of Pounding and Restrainers on Seismic Response of Multiple-Frame Bridges." *Journal of Structural Engineering* 128 (7): 860–869. https://doi.org/10.1061/(ASCE)0733-9445(2002)128:7(860).

Goldsmith, W. 1960. *Impact - The Theory and Physical Behaviour of Colliding Solids*. London, UK: Edward Arnold LTD.

Guo, A., L. Cui, and H. Li. 2012. "Impact Stiffness of the Contact-Element Models for the Pounding Analysis of Highway Bridges: Experimental Evaluation." *Journal of Earthquake Engineering* 16 (8): 1132–1160. https://doi.org/10.1080/13632469.2012.693243.

Hao, H., K. Bi, N. Chouw, and W. Ren. 2013. "State-Of-The-Art Review on Seismic Induced Pounding Response of Bridge Structures." *Journal of Earthquake and Tsunami* 7 (3): 1350019. https://doi.org/10.1142/S179343111350019X.

Jalayer, F., and J. Beck. 2008. "Effects of Two Alternative Representations of Ground-Motion Uncertainty on Probabilistic Seismic Demand Assessment of Structures." *Earthquake Engineering & Structural Dynamics* 37 (1): 61–79. https://doi.org/10.1002/eqe.745.

Jankowski, R. 2005. "Non-Linear Viscoelastic Modelling of Earthquake-Induced Structural Pounding." *Earthquake Engineering & Structural Dynamics* 34 (6): 595–611. https://doi.org/10.1002/eqe.434.

Jankowski, R. 2006. "Pounding Force Response Spectrum Under Earthquake Excitation." *Engineering Structures* 28 (8): 1149–1161. https://doi.org/10.1016/j.engstruct.2005.12.005.

Jankowski, R. 2008. "Earthquake-Induced Pounding Between Equal Height Buildings with Substantially Different Dynamic Properties." *Engineering Structures* 30 (10): 2818–2829. https://doi.org/10.1016/j.engstruct.2008.03.006.

Jeng, V., and W. Tzeng. 2000. "Assessment of Seismic Pounding Hazard for Taipei City." *Engineering Structures* 22 (5): 459–471. https://doi.org/10.1016/S0141-0296(98)00123-0.

Kanai, K. 1957. "Semi-Empirical Formula for the Seismic Characteristics of the Ground." *Bulletin of the Earthquake Research Institute* 35 (2): 309–325. https://repository.dl.itc.u-tokyo.ac.jp/record/33949/files/ji0352002.pdf .

Kim, M. K., J. H. Kim, G. Mosqueda, and A. Sarebanhab. 2015. "Effects of Moat Wall Impact on the Seismic Response of Base Isolated Nuclear Power Plants."

Komodromos, P. 2008. "Simulation of the Earthquake-Induced Pounding of Seismically Isolated Buildings." *Computers & Structures* 86 (7–8): 618–626. https://doi.org/10.1016/j.compstruc.2007.08.001.

Komodromos, P., P. C. Polycarpou, L. Papaloizou, and M. C. Phocas. 2007. "Response of Seismically Isolated Buildings Considering Poundings." *Earthquake Engineering & Structural Dynamics* 36 (12): 1605–1622. https://doi.org/10.1002/eqe.692.

Li, H., G. Sun, and Y. Ren. 2008. "A Note on the Stationary Model of Earthquake Induced Ground Motion with a Hu Spectrum." In *Proceedings of the14th World Conference on Earthquake Engineering*, 03-0050. Beijing:[sn].

Lopez-Garcia, D., and T. Soong. 2009. "Assessment of the Separation Necessary to Prevent Seismic Pounding Between Linear Structural Systems." *Probabilistic Engineering Mechanics* 24 (2): 210–223. https://doi.org/10.1016/j.probengmech.2008.06.002.

Maison, B. F., and K. Kasai. 1992. "Dynamics of Pounding When Two Buildings Collide." *Earthquake Engineering & Structural Dynamics* 21 (9): 771–786. https://doi.org/10.1002/eqe.4290210903.

Masroor, A., and G. Mosqueda. 2012. "Experimental Simulation of Base-Isolated Buildings Pounding Against Moat Wall and Effects on Superstructure Response." *Earthquake Engineering & Structural Dynamics* 41 (14): 2093–2109. https://doi.org/10.1002/eqe.2177.

Mckay, M. D., R. J. Beckman, and W. J. Conover. 1979. "Comparison of Three Methods for Selecting Values of Input Variables in the Analysis of Output from a Computer Code." *Technometrics* 21 (2): 239–245. https://doi.org/10.1080/00401706.1979.10489755.

Moehle, J. P., and S. A. Mahin. 1991. "Observations on the Behavior of Reinforced Concrete Buildings During Earthquakes." *Special Publication* 127:67–90. https://doi.org/10.14359/3007.

Moré, J. J. 1978. "The Levenberg-Marquardt Algorithm: Implementation and Theory." In *Numerical Analysis* [Lecture Notes in Mathematics], Vol. 630. Berlin, Heidelberg: Springer. https://doi.org/10.1007/BFb0067700.

Muthukumar, S., and R. Desroches. 2006. "A Hertz Contact Model with Non-Linear Damping for Pounding Simulation." *Earthquake Engineering & Structural Dynamics* 35 (7): 811–828. https://doi.org/10.1002/eqe.557.

Nagarajaiah, S., and X. Sun. 2001. "Base-Isolated FCC Building: Impact Response in Northridge Earthquake." *Journal of Structural Engineering* 127 (9): 1063–1075. https://doi.org/10.1061/(ASCE)0733-9445(2001)127:9(1063).

Otsuka, H., S. Unjoh, T. Terayama, J. Hoshikuma, and K. Kosa. 1996. "Damage to Highway Bridges by the 1995 Hyogoken Nanbu Earthquake and the Retrofit of Highway Bridges in Japan." In *Proceedings of the 3rd US Japan Workshop on Seismic Retrofit of Bridge*. Osaka, Japan.

Pantelides, C., and X. Ma. 1998. "Linear and Nonlinear Pounding of Structural Systems." *Computers & Structures* 66 (1): 79–92. https://doi.org/10.1016/S0045-7949(97)00045-X.

Patelli, E. 2016. "COSSAN: A Multidisciplinary Software Suite for Uncertainty Quantification and Risk Management." In *Handbook of Uncertainty Quantification*, edited by Roger Ghanem, David Higdon, and Houman Owhadi, 1–69. Cham: Springer International Publishing. https://doi.org/10.1007/978-3-319-12385-1_59.

Patelli, E., H. J. Pradlwarter, and G. I. Schuëller. 2010. "Global Sensitivity of Structural Variability by Random Sampling." *Computer Physics Communications* 181 (12): 2072–2081. https://doi.org/10.1016/j.cpc.2010.08.007.

Patelli, E., S. Tolo, H. George-Williams, J. Sadeghi, R. Rocchetta, M. De Angelis, and M. Broggi, 2018. "Opencossan 2.0: An Efficient Computational Toolbox for Risk, Reliability and Resilience Analysis." In *Proceedings of the Joint ICVRAM ISUMA UNCERTAINTIES conference*. http://icvramisuma2018.org/cd/web/PDF/ICVRAMISUMA2018-0022.PDF.

Pellissetti, M., H. Keßler, F. Laudarin, D. Altieri, A. Nykyforchyn, E. Patelli, and J.-U. Klügel. 2017. "Statistical Analysis of Impact Forces and Permanent Deformations of Fuel Assembly Spacer Grids in the Context of Seismic Fragility." 24th Conference on Structural Mechanics in Reactor Technology, Busan, South Korea.

Penzien, J. 1997. "Evaluation of Building Separation Distance Required to Prevent Pounding During Strong Earthquakes." *Earthquake Engineering & Structural Dynamics* 26 (8): 849–858. https://doi.org/10.1002/(SICI)1096-9845(199708)26:8<849:AID-EQE680>3.0.CO;2-M.

Saltelli, A., M. Ratto, T. Andres, F. Campolongo, J. Cariboni, D. Gatelli, M. Saisana, and S. Tarantola. 2008. *Global Sensitivity Analysis: The Primer*. Chichester, England: John Wiley & Sons Ltd. https://doi.org/10.1002/9780470725184 .

Sobol, I. M. 1993. "Sensitivity Estimates for Nonlinear Mathematical Models." *Mathematical Modelling and Computational Experiments* 1:407–414. http://www.andreasaltelli.eu/file/repository/sobol1993.pdf .

Tajimi, H. 1960. "A Statistical Method of Determining the Maximum Response of a Building Structure During an Earthquake." In *Proceedings of the 2nd World Conference on Earthquake Engineering*, 781–797. Tokyo and Kyoto, Japan.

Tubaldi, E., M. Barbato, and S. Ghazizadeh. 2012. "A Probabilistic Performance-Based Risk Assessment Approach for Seismic Pounding with Efficient Application to Linear Systems." *Structural Safety* 36:14–22. https://doi.org/10.1016/j.strusafe.2012.01.002.

Tubaldi, E., F. Freddi, and M. Barbato. 2016. "Probabilistic Seismic Demand Model for Pounding Risk Assessment." *Earthquake Engineering & Structural Dynamics* 45 (11): 1743–1758. https://doi.org/10.1002/eqe.2725.

Van Mier, J. G., A. F. Pruijssers, H. W. Reinhardt, and T. Monnier. 1991. "Load-Time Response of Colliding Concrete Bodies." *Journal of Structural Engineering* 117 (2): 354–374. https://doi.org/10.1061/(ASCE)0733-9445(1991)117:2(354).

Vega, J., I. Del Rey, and E. Alarcon. 2009. "Pounding Force Assessment in Performance-Based Design of Bridges." *Earthquake Engineering & Structural Dynamics* 38 (13): 1525–1544. https://doi.org/10.1002/eqe.916.

Wu, Q., T. Wang, H. Ge, and H. Zhu. 2019. "Dimensional Analysis of Pounding Response of an Oscillator Based on Modified Kelvin Pounding Model." *Journal of Aerospace Engineering* 32 (4): 04019039. https://doi.org/10.1061/(ASCE)AS.1943-5525.0001018.

Yaghmaei-Sabegh, S., and N. Jalali-Milani. 2012. "Pounding Force Response Spectrum for Near-Field and Far-Field Earthquakes." *Scientia Iranica* 19 (5): 1236–1250. https://doi.org/10.1016/j.scient.2012.07.012.

Zhai, C., S. Jiang, and Z. Chen. 2014. "Dimensional Analysis of the Pounding Response of an Oscillator Considering Contact Duration." *Journal of Engineering Mechanics* 141 (4): 04014138. https://doi.org/10.1061/(ASCE)EM.1943-7889.0000858.

Zheng, Y., X. Xiao, L. Zhi, and G. Wang. 2015. "Evaluation on Impact Interaction Between Abutment and Steel Girder Subjected to Nonuniform Seismic Excitation." *Shock and Vibration* 2015:1–14. https://doi.org/10.1155/2015/981804.

Zito, M., R. Nascimbene, P. Dubini, D. D'angela, and G. Magliulo. 2022. "Experimental Seismic Assessment of Nonstructural Elements: Testing Protocols and Novel Perspectives." *Buildings* 12 (11): 1871. https://doi.org/10.3390/buildings12111871.

Appendix. Seismic Model

This study employs the Atkinson and Silva ground motion model (Atkinson and Silva 2000) in conjunction with the stochastic point source method of Boore (2003) for the generation of earthquake ground motion time history samples. The seismological parameters that define the adopted stochastic model are the moment magnitude, M_w, and the epicentral (source-to-site) distance, R, which are modelled as random variables. The magnitude follows a truncated Gutenberg-Richter probability density function (PDF) that is defined as:

$$f_M(m_s) = \frac{\beta \cdot e^{-\beta \cdot (m_w - m_{w,0})}}{1 - e^{-\beta \cdot (m_{w,\max} - m_{w,0})}} \tag{10}$$

This study assumes $m_{w,0} = 5$, $m_{w,\max} = 8$, and $\beta = 2.303$ (Au and Beck 2003), which provide a Gutenberg-Richter PDF that is consistent with the California seismicity. The source-to-site distance is modelled according to the following PDF:

$$f_R(r) = \begin{cases} \frac{2r}{r_{\max}} & \text{if } 0 \le r \le r_{\max} \\ 0 & \text{otherwise} \end{cases} \tag{11}$$

which implies a source producing random earthquakes with a uniform distribution over a circle centred around the site with a radius $r_{\max} = 50$ km (Au and Beck 2003), outside which the seismic effects are considered negligible. The site-dependent mean annual frequency of occurrence for the seismic events, ν_0, is assumed here equal to 0.25 year^{-1}.

The record-to-record variability for a given combination of M_w and R is modelled by generating the seismic signal from a Gaussian white-noise process. The generated white-noise is modulated by an envelope function, $e(t)$, and the resulting signal $z(t) = e(t) \cdot w_n(t)$ is subject to a Fourier transformation to obtain the normalized signal $\bar{z}(f)$ in the frequency domain. The synthetic ground motion record is finally computed through an inverse Fourier transformation of the signal $\bar{z}(f) \cdot \varepsilon_{\text{mod}} \cdot A(f)$, where $A(f)$ denotes the radiation spectrum. Following (Jalayer and Beck 2008), a random amplification factor, ε_{mod}, is introduced to amplify the radiation spectra. This factor is assumed to be lognormally distributed with parameters $\lambda = \mu_{\log(\varepsilon_{\text{mod}})} = 0$ and $\xi = \sigma_{\log(\varepsilon_{\text{mod}})} = 0.5$. Both the radiation spectrum and the time-envelope function depend on the values of M_w and R, i.e., they change from record sample to record sample. Figure A1 shows the radiation spectra and envelope functions for different values of m_w and $r = 20$ km.

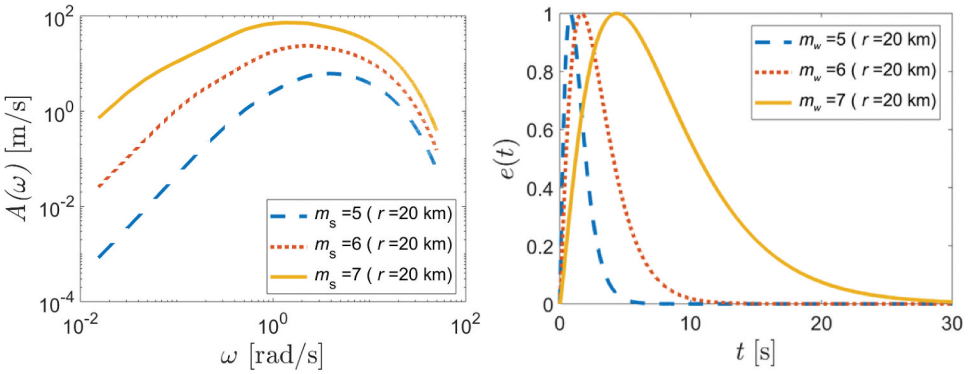

Figure A1. Radiation Fourier spectra (left) and the time-envelope functions (right) for r = 20 km and different *M* values.